

The energy dependence of burst oscillations from the accreting millisecond pulsar XTE J1814-338

Anna L. Watts¹ and Tod E. Strohmayer²

¹ *Max Planck Institut für Astrophysik, Karl-Schwarzschild-Str.1, 85741 Garching, Germany; anna@mpa-garching.mpg.de*

² *Exploration of the Universe Division, NASA Goddard Space Flight Center, Greenbelt, MD 20771, USA; stroh@milkyway.gsfc.nasa.gov*

25 January 2019

ABSTRACT

The nature of the asymmetry that gives rise to Type I X-ray burst oscillations on accreting neutron stars remains a matter of debate. Of particular interest is whether the burst oscillation mechanism differs between the bursting millisecond pulsars and the non-pulsing systems. One means to diagnose this is to study the energy dependence of the burst oscillations: here we present an analysis of oscillations from 28 bursts observed during the 2003 outburst of the accreting millisecond pulsar XTE J1814-338. We find that the fractional amplitude of the burst oscillations falls with energy, in contrast to the behaviour found by Muno et al. (2003) in the burst oscillations from a set of non-pulsing systems. The drop with energy mirrors that seen in the accretion-powered pulsations; in this respect XTE J1814-338 behaves like the other accreting millisecond pulsars. The burst oscillations show no evidence for either hard or soft lags, in contrast to the persistent pulsations, which show soft lags of up to 50 μ s. The fall in amplitude with energy is inconsistent with current surface mode and simple hot spot models of burst oscillations. We discuss improvements to the models and uncertainties in the physics that might resolve these issues.

Key words: binaries: general—stars:individual (XTE J1814-338)—stars:neutron—stars:rotation—X-rays:binaries—X-rays:bursts

1 INTRODUCTION

Of the ≈ 160 known non-pulsing neutron star Low Mass X-Ray Binaries (LMXBs), nearly half exhibit Type I X-ray bursts due to unstable nuclear burning of accreting material. High frequency modulations of the X-ray lightcurve, known as burst oscillations, have now been detected in the bursts from twelve of these systems (see the recent review by Strohmayer & Bildsten (2006)). Of the seven known accreting millisecond pulsars, three exhibit bursts. Two of these systems, SAX J1808.4-3658 (hereafter J1808) and XTE J1814-338 (hereafter J1814), have burst oscillations.

For the pulsars, the burst oscillation frequency is at or very close to the known spin frequency of the star (Chakrabarty et al. 2003; Strohmayer et al. 2003). This suggests that the rotation modulates an asymmetry on the burning surface that is near-stationary in the corotating frame. For the non-pulsars the situation is less clear, because there is no independent measure of the spin frequency. The fact that the frequency is highly stable from burst to burst, however (Strohmayer et al. 1998; Muno, Özel & Chakrabarty 2002), implies that there is at least a strong dependence on stellar spin. The detection of

highly coherent oscillations lasting several hundred seconds during a superburst from the LMXB 4U 1636-356 adds further support to this hypothesis (Strohmayer & Markwardt 2002a).

The precise nature of the brightness asymmetry is as yet unclear. The simplest possibility is uneven distribution of fuel, leading to patchy burning. For the pulsars we know that initial fuel distribution is asymmetric, but the fuel could spread rapidly over the surface. For the non-pulsars there is no evidence of asymmetric fuel deposition, although there are several mechanisms that might render this process (and the associated pulsations) undetectable (Brainerd & Lamb 1987; Kylafis & Klimmis 1987; Wood, Ftaclas & Kearney 1988; Mészáros, Riffert & Berthiaume 1988; Cumming, Zweibel & Bildsten 2001; Titarchuk, Cui & Wood 2002). Alternate mechanisms that do not rely on asymmetric fuel distribution include the development of vortices driven by the Coriolis force (Spitkovsky, Levin & Ushomirsky 2002), or global modes in the burning surface layers (McDermott & Taam 1987; Lee 2004; Heyl 2004; Lee & Strohmayer 2005; Cumming 2005; Piro & Bildsten 2005).

One means of diagnosing the nature of the asymme-

try is to study the energy dependence of the burst oscillations. Munro, Özel & Chakrabarty (2003) examined the energy dependence expected for a simple hot spot model, generating simulated *Rossi X-ray Timing Explorer* (RXTE) Proportional Counter Array (PCA) lightcurves for neutron stars with a circular uniform temperature hot spot on a cooler background. Doppler effects due to the star's rotation lead naturally to a rise in fractional amplitude with energy in the 3-20 keV band. The hot spot model also predicts soft lags. Models where the burst oscillations are caused by surface modes also predict a rise in fractional amplitude with energy (Heyl 2005; Piro & Bildsten 2006). In most cases the mode models predict soft lags, although Lee & Strohmayer (2005) found hard lags for a restricted subset of possible geometries.

The most comprehensive study to date of burst oscillations from the non-pulsing LMXBs, using RXTE PCA data, found that fractional amplitude rises with energy over the 3-20 keV waveband (Munro, Özel & Chakrabarty 2003). The authors show that the observations are compatible with the simple hot spot model if the bulk of the stellar surface (away from the hot spot) emits in the lower part of the PCA waveband. The data are also compatible with surface mode models (Piro & Bildsten 2006), provided that the required amplitudes can be excited.

Munro et al. also examined whether there were phase lags between soft and hard photons. For most bursts the data were consistent with there being no phase lag; for 13 of 54 bursts studied the data were inconsistent at the 90% confidence level with being constant. In these bursts the trend was for the hard photons to lag the soft photons by up to 0.12 cycles, whereas both simple hot spot and mode models predict soft lags. The authors considered several mechanisms that might reverse a soft lag. They concluded that inverse Compton scattering of soft photons to higher energies by a hot corona of electrons was the most likely candidate (Miller 1995). The observational implications of such a corona, however, and its behaviour during a burst, remain to be worked out in detail.

To date there has been no study reporting the energy dependence of the burst oscillations of the accreting millisecond pulsars. Given the possibility that the burst oscillation mechanism may differ from that operating in the non-pulsing sources, this is clearly an omission. In this paper we attempt to rectify this by presenting an analysis of the energy dependence of the burst oscillations of J1814.

The source was first detected in outburst on 2003 June 3 by the RXTE Galactic bulge monitoring campaign. Its status as a millisecond pulsar was confirmed by a longer observation on June 5 (Markwardt & Swank 2003). The pulsar has a spin frequency of 314.36 Hz, resides in a binary with orbital period 4.275 hr, and has a minimum companion mass of $\approx 0.15M_{\odot}$ (Markwardt, Strohmayer & Swank 2003). The binary orbit is the widest of the seven known accreting millisecond pulsars. J1814 remained in outburst until mid-July 2003, and in this time 28 Type I X-ray bursts were observed, all with detectable burst oscillations at the spin frequency (Strohmayer et al. 2003). The bursts show significant harmonic content, which could be used to constrain the equation of state and the system geometry (Bhattacharyya et al. 2005). A detailed study by Watts, Strohmayer & Markwardt (2005) found that there

is no evidence for fractional amplitude variation or frequency shifts in any of the bursts apart from the one burst that appears to show photospheric radius expansion. For most of the bursts, fractional amplitude is consistent with that of the persistent pulsations, although there is a small population of bursts with amplitudes that are substantially lower. For the first harmonic, substantial differences between the burst and accretion-powered oscillations indicate that hot spot geometry is not the only factor giving rise to harmonic content in the latter. There are however no detectable phase shifts between the burst and accretion-powered pulsations (Strohmayer et al. 2003), suggesting a model where the presence of the magnetic field somehow leads to a temperature asymmetry centered on the polar cap when the burst ignites (by allowing additional fuel build-up, for example). In this complementary study we test the models further by examining the energy dependence of the burst oscillations, comparing the behaviour to that of the accretion-powered pulsations. Section 2 details our method of analysis and our results. In Section 3 we discuss our findings in the light of current burst oscillation models, and outline areas for future theoretical study.

2 DATA ANALYSIS

2.1 Methodology

Almost all of the PCA data for the outburst is event mode data with 125 μ s time resolution and 64 energy bins covering the range 2 - 120 keV. The exception is the first burst, which was recorded in GoodXenon mode, which has higher time and energy resolution (1 μ s and 256 energy bins). Event mode data overruns, which are often seen in the bursts of brighter sources, were not seen in any of the J1814 bursts. The data were barycentered prior to analysis, using the JPL DE405 ephemeris and the source position determined from PCA scans (Markwardt & Swank 2003; Krauss et al. 2005).

Computation of fractional amplitudes is done in two ways. We start by using the Z_n^2 statistic (Buccheri et al. 1983; Strohmayer & Markwardt 2002b). This measure is very similar to the standard power spectrum computed from a Fourier transform, but does not require that the event data be binned. It is defined as

$$Z_n^2 = \frac{2}{N} \sum_{k=1}^n \left[\left(\sum_{j=1}^N \cos k\phi_j \right)^2 + \left(\sum_{j=1}^N \sin k\phi_j \right)^2 \right] \quad (1)$$

where n is the number of harmonics summed (we use $n = 1$ throughout this paper), N is the total number of photons, and j is an index applied to each photon. The phase ϕ_j calculated for each photon is

$$\phi_j = 2\pi \int_{t_0}^{t_1} \nu(t) dt \quad (2)$$

where $\nu(t)$ is the frequency model and t_j is the arrival time of the photon relative to some reference time. We use a frequency model in which the intrinsic spin rate is modified by orbital Doppler shifts using the best fit orbital ephemeris.

Given a measured Z_n^2 , which we call Z_m , the probability of the true signal power lying between 0 and Z_s is given by:

$$f(Z_s : Z_m) = \exp \left[-\frac{Z_m + Z_s}{2} \right] \left[\sum_{k=0}^{\infty} \sum_{l=0}^{k+n-1} \frac{(Z_s)^k (Z_m)^l}{l!k!2^{k+1}} \right] \quad (3)$$

(Groth 1975; Vaughan et al. 1994). We take the best estimate for Z_s to be that for which $f(Z_s : Z_m) = 0.5$. Given this Z_s the RMS fractional amplitude r is then given by

$$r = \left(\frac{Z_s}{N} \right)^{1/2} \left(\frac{N}{N - N_b} \right) \quad (4)$$

where N_b is the number of photons due to background accumulated in the energy band of interest during the observation period. N_b is estimated using the standard FTOOLS routine `pcabackest` and the PCA background models.

The second method used is to generate a folded pulse profile (using the frequency model) and then fit a sinusoidal model with as many harmonics as necessary. We use this method to check the fractional amplitudes computed using the Z_n^2 statistic. Pulse profile fitting also allows us to calculate phase shifts between the different energy bands, something that is not possible using the Z_n^2 statistic alone. A more extensive discussion of both of these methods is given in Section 2.1 of Watts, Strohmayer & Markwardt (2005).

The other issue to consider when computing fractional amplitudes for pulsar burst oscillations is that the accretion process may continue during the bursts. If this is the case then the measured fractional amplitude will contain contributions from both the burst process and the accretion process:

$$r = \frac{r_{\text{bur}} N_{\text{bur}} + r_{\text{acc}} N_{\text{acc}}}{N_s} \quad (5)$$

N_{bur} and N_{acc} are the number of source photons arising from the burst and accretion processes respectively, with r_{bur} and r_{acc} being the fractional amplitudes of the two different processes. The total number of source photons is $N_s = N_{\text{bur}} + N_{\text{acc}}$. Since we are not always in the regime where $N_{\text{bur}} \gg N_{\text{acc}}$ we will need to estimate N_{acc} and r_{acc} in order to check whether r_{bur} differs substantially from that measured. We do this in Section 2.2.

2.2 Accretion-powered pulsations

We start by folding together data from the whole outburst to generate a high resolution plot of amplitude and phase lags against energy for the accretion-powered pulsations. Figure 1 shows the behaviour of amplitude against energy, for both the fundamental and first harmonic. There is a clear drop in amplitude with energy for the fundamental, of about 2% RMS over the 2-20 keV band. The amplitude of the first harmonic, by contrast, varies little with energy. Figure 2 shows the phase shifts between the different energy bands for the fundamental. Soft lags of up to 50 μs (≈ 0.015 cycles) develop over the range 2-7 keV, with the lags levelling off at higher energies. The same behaviour is seen in the phase shifts computed using the first harmonic.

This behaviour mirrors that seen in the

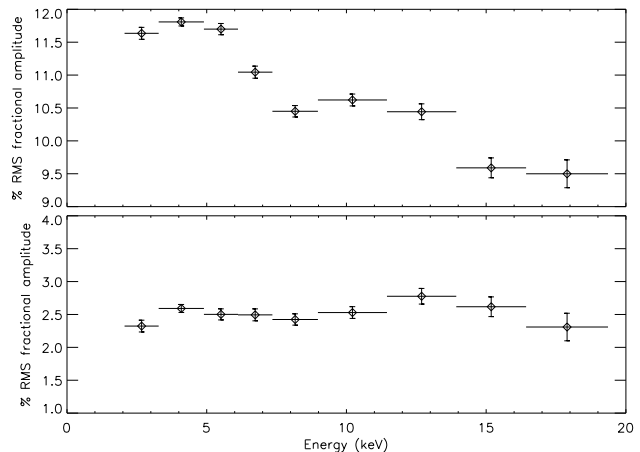


Figure 1. Dependence of fractional amplitude on energy for the accretion-powered pulsations, computed from a folded profile using data from the whole outburst. The fundamental (top panel) shows a clear drop in amplitude with energy. The amplitude of the first harmonic, by contrast (lower panel) shows little change with energy.

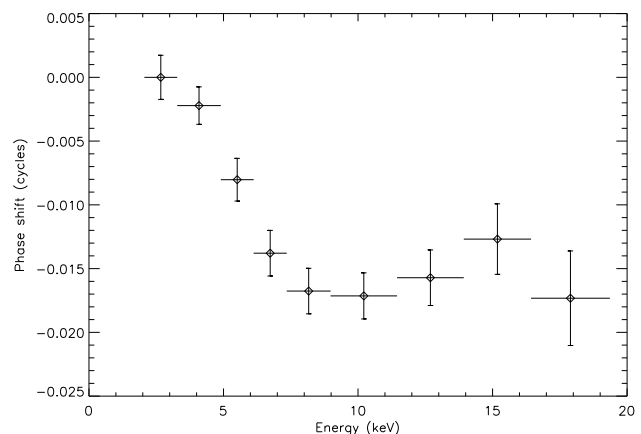


Figure 2. Phase shifts compared to the phase for the lowest energy band (2-3.3 keV) for the accretion-powered pulsations. Negative values indicate that the pulse profile in the band being studied leads the profile in the lowest energy band, with 0.01 cycles corresponding to 31.8 μs . The phase shifts were computed by folding together data from the whole outburst.

accretion-powered pulsations of the other millisecond pulsars: J1808 (Cui, Morgan & Titarchuk 1998; Gierliński, Done & Barret 2002), XTE J0929-314 (Galloway et al. 2002), XTE J1807-294 (Kirsch et al. 2004), IGR J00291+5934 (Galloway et al. 2005) and XTE J1751-305 (Gierliński & Poutanen 2005) all show a drop of fractional amplitude with energy within the PCA waveband. The other sources also show soft lags, although at only 50 μs the J1814 lags are smaller than those measured for the other systems. Detailed spectral modelling for J1808 by Gilfanov et al. (1998), Gierliński, Done & Barret (2002) and Poutanen & Gierliński (2003) suggests that a hard Comptonized component due to boundary layer emission precedes a softer blackbody component due to a hot spot at

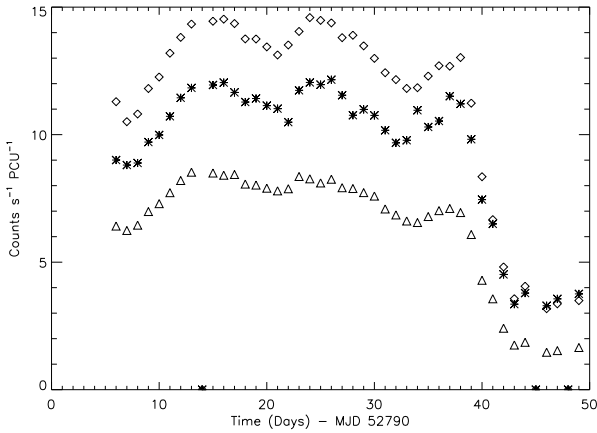


Figure 3. Daily average count rate (excluding bursts) in different energy bands, corrected for background. Stars: 2-5 keV. Diamonds: 5-10 keV. Triangles: 10-20 keV.

the footpoint of the accretion channel. The boundary layer is larger than the underlying hot spot, leading to a lower fractional amplitude at higher energies. Similar detailed modelling for J1814, which has a harder spectrum than J1808 (Markwardt, Strohmayer & Swank 2003), has yet to be done.

In order to correct for the accretion contribution recorded during the bursts, we also need to know whether the properties of the persistent pulsations vary over the course of the outburst. Figure 3 shows the change in the count rate (excluding bursts) for the three energy bands 2-5 keV, 5-10 keV, and 10-20 keV. The evolution of fractional amplitude (at the fundamental frequency) is shown in Figure 4. The trend of amplitude dropping with energy is apparent over the whole outburst, although the magnitude of the drop does vary between 1% and 3% RMS over the outburst. The phase shifts between the different energy bands are shown in Figure 5. Again the soft lags persist throughout, but get noticeably larger at the end of the outburst, when the accretion rate drops. It would be interesting to see if such a variation in phase lag with accretion rate is detected in any of the other millisecond pulsars.

2.3 Burst oscillations

The proportion of photons in the different energy bands for each of the bursts is shown in Figure 6. For most of the bursts the proportions are very similar. For the six faintest bursts, the proportions in the higher energy bands drop, as might be expected. Similarly, for the brightest burst, the proportion in the highest energy band rises. We define the duration of the burst as to be the time for which the count rate in a given energy band exceeds the ambient count rate by a factor of 1.5. Using this definition, burst duration is shorter at higher energies.

We start by considering each of the bursts separately, computing fractional amplitudes and phase shifts for the three energy bands 2-5 keV, 5-10 keV and 10-20 keV. The fractional amplitudes (at the fundamental frequency) for all of the bursts are shown in Figure 7, and summarized in

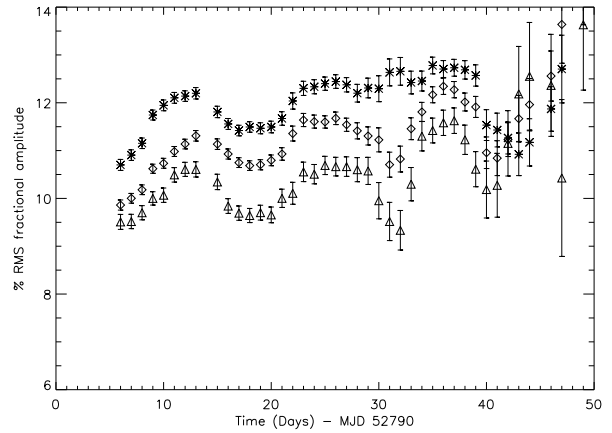


Figure 4. Fractional amplitudes for the accretion-powered pulsations for different energy bands, showing the variations over the outburst. Stars: 2-5 keV. Diamonds: 5-10 keV. Triangles: 10-20 keV. Each point is computed by folding data for a 5 day period starting on the day indicated. The drop in fractional amplitude with energy persists throughout the outburst, although the magnitude of the change does vary, particularly at the point where the accretion rate starts to drop.

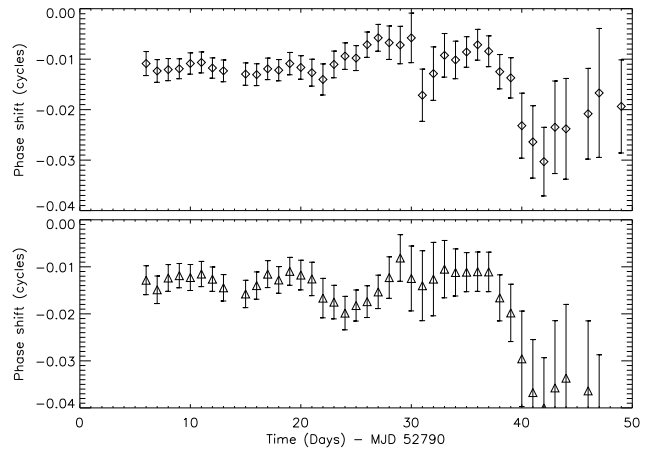


Figure 5. Phase shifts compared to the phase for the 2-5 keV band for the accretion-powered pulsations, showing the evolution over the outburst. Top: 5-10 keV. Bottom: 10-20 keV. Negative values indicate that the pulse profile in the band being studied leads the profile in the 2-5 keV band, with 0.01 cycles corresponding to $31.8\mu\text{s}$. Each point is computed by folding data for a 5 day period starting on the day indicated.

columns 2-4 of Table 1 (for more general data on each burst see Table 1 of Watts, Strohmayer & Markwardt (2005)). More detailed plots for four example bursts are shown in Figure 8. We find that burst amplitude is lower in the 10-20 keV band than in the 2-5 keV band for 25 of the 28 bursts. Treating each burst as an independent test, we find that we can rule out the hypothesis that fractional amplitude is constant with energy at a level greater than 3σ . The hypothesis that fractional amplitude rises with energy can be ruled out with an even higher degree of confidence.

The phase shifts between the different energy bands for

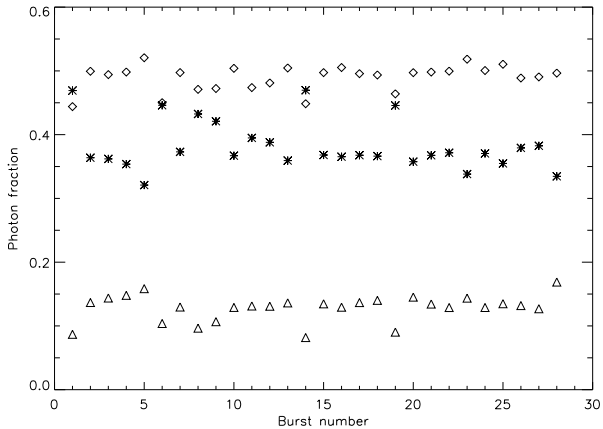


Figure 6. Proportion of photons in the different energy bands during each burst (corrected for background and an estimate of the accretion-related emission). Proportions are roughly constant, although for the faintest bursts (1, 6, 8, 9, 14 and 19, see Figure 4 of Watts et al. 2005) the proportion of photons in the highest energy bands drops. For the final, brightest burst, the proportion in the highest energy band is higher. Stars: 2-5 keV. Diamonds: 5-10 keV. Triangles: 10-20 keV.

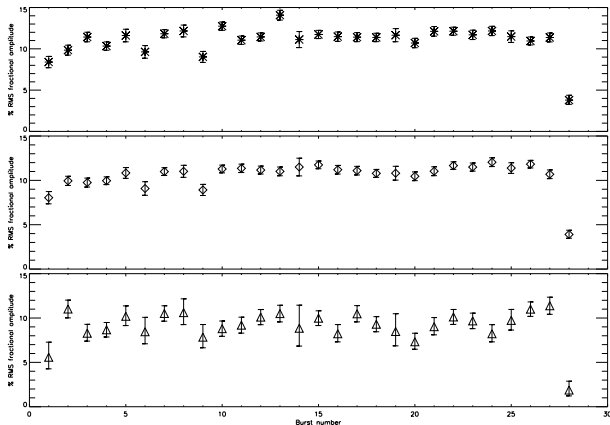


Figure 7. Burst RMS fractional amplitude (%) for different energy bands, at the fundamental frequency of the pulsar. *Top:* 2-5 keV. *Middle:* 5-10 keV. *Bottom:* 10-20 keV. The scales on each plot are the same to make clear the general drop in fractional amplitude with energy.

each burst are shown in Figure 9. There is no evidence for either hard or soft lags; the data are compatible with there being no phase shift.

In order to verify these results, we folded together data from all of the bursts to generate a combined profile. We find a drop of fractional amplitude with energy of $\approx 3\%$ RMS over the 2-20 keV band, a steeper drop than that seen in the persistent pulsations (Figure 10). The phase shifts of the combined profile, for two energy binnings, are shown in Figure 11. The data are consistent with there being no phase shift, and we can rule out at the 3σ level hard or soft lags of greater than 0.015 cycles over the 2-20 keV band. We

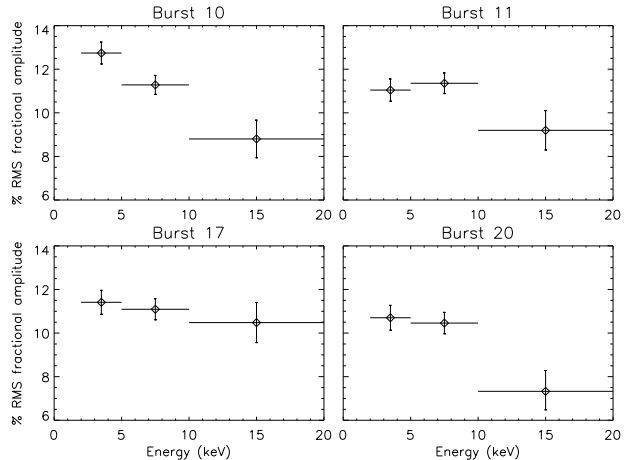


Figure 8. Energy dependence of fractional amplitude for four example bursts. Burst numbers accord with those in Table 1 of this paper and Table 1 of Watts, Strohmayer & Markwardt (2005). For bursts 10 and 17 a linear relation between fractional amplitude and energy is a good fit, although the gradients are very different. For bursts 11 and 20 the amplitude is relatively constant between the 2-5 and 5-10 keV bands, dropping only in the 10-20 keV band.

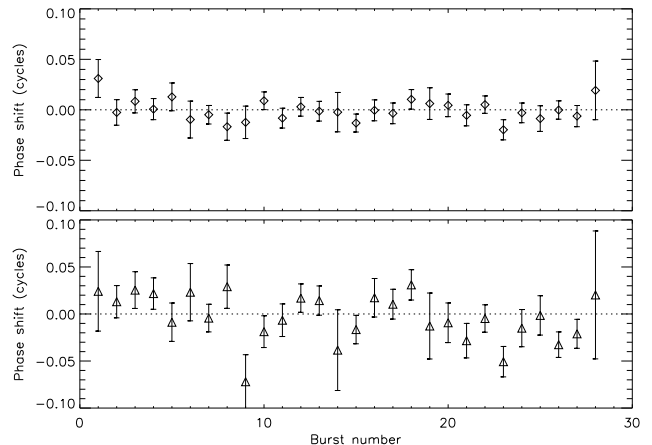


Figure 9. Phase shifts compared to the phase for the 2-5 keV band for the bursts. *Top:* 5-10 keV. *Bottom:* 10-20 keV. Negative values indicate that the pulse profile in the band being studied leads the profile in the 2-5 keV band, with 0.01 cycles corresponding to $31.8\mu\text{s}$.

would have been sensitive to lags of the magnitude seen in the accretion-powered pulsations were such lags present.

3 DISCUSSION

The burst oscillations of J1814 exhibit a drop in fractional amplitude with energy of a few percent RMS across the 2-20 keV band. In addition the bursts show no evidence for phase shifts between soft and hard photons; we can rule out at the 3σ level shifts greater than 0.015 cycles over the 2-20 keV band. In this section we discuss these results in the context of the various burst oscillation models.

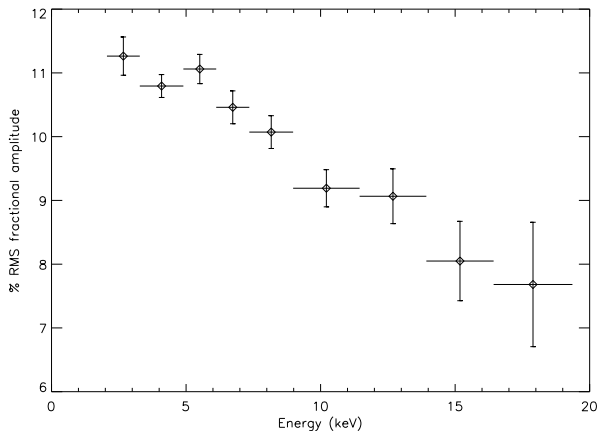


Figure 10. The dependence of fractional amplitude on energy for the bursts, computed from a folded profile of data from all of the bursts. No attempt has been made to correct for the accretion contribution (see discussion in the text).

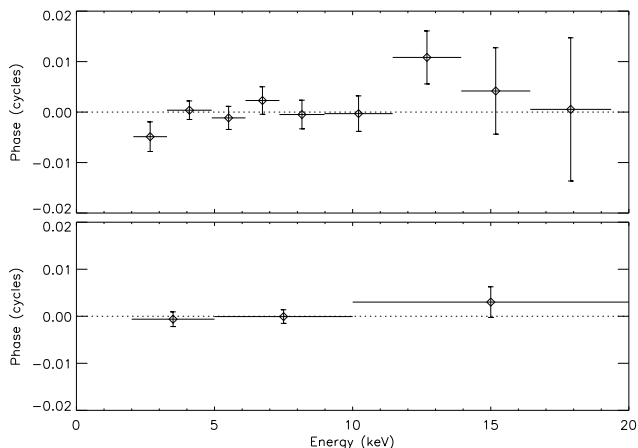


Figure 11. Phases calculated for the folded set of bursts, relative to the best fitting constant phase. The top panel shows a higher energy resolution than the lower panel. Both sets of data are consistent with there being no phase shift between the different energy bands. Note that 0.01 cycles corresponds to $31.8\mu\text{s}$.

3.1 Consistency with existing burst oscillation models

We start by considering models where surface modes cause the brightness asymmetry. The mode models discussed by Heyl (2005); Lee & Strohmayer (2005) and Piro & Bildsten (2006) all predict a rise of amplitude with energy, although the gradient of the rise depends on various neutron star parameters. Since we can rule out a rise, or even a constant amplitude, with a high degree of confidence, the amplitude data are inconsistent with these models. The phase lag data do not provide any additional constraint, since the models of (for example) Lee & Strohmayer (2005) predict anything from hard lags of 0.04 cycles to soft lags of 0.1 cycle depending on the neutron star properties. Although we can rule out lags greater than 0.015 cycles there are still models that would fit the phase lag data.

What about current hot spot models? The simple one-temperature hot spot models studied by Munro, Özel & Chakrabarty (2003) also predict a rise of amplitude with energy, although again the magnitude of the rise depends on the neutron star properties. The models studied by Munro et al. also predict soft lags of least 0.02 cycles over the RXTE waveband. Any phase lags present in the burst oscillations of J1814 are smaller than this limit.

We are therefore left with several options. One possibility is that the burst oscillation properties are consistent with existing mode/hot spot models but are masked by the presence of accretion-powered pulsations. We examine this in more detail in Section 3.2, and show that the accretion process would have to be disrupted substantially by the bursts to explain the observations. A second option is that existing models are not adequate to explain the observations. In Section 3.3 we examine whether a hot spot with a temperature gradient might lead to consistency with the observations.

3.2 Masking by the accretion pulsations

Unless the accretion process is completely disrupted by the burst, the measured fractional amplitude will contain contributions from both accretion and burst pulsations. Separating the two contributions is not trivial because in this source they are phase-locked (Strohmayer et al. 2003). The persistent pulsations of J1814 do indeed show a drop in fractional amplitude with energy of 1-3% RMS over the 2-20 keV energy band (during the main portion of the outburst), so masking is not inconceivable. To proceed we need to estimate the magnitude of the accretion contribution to Equation (5).

We start by making the simple assumption that both the accretion rate and the amplitude/energy relation of the accretion-powered pulsations remain in their pre-burst state, as presented in Section 2.2, during a burst. Columns 5-7 of Table 1 give an estimate of the ratio of accretion to burst photons over the duration of the burst, computed from the daily average accretion rate at the time of the burst. In Columns 8-10 we combine this estimate with the daily average fractional amplitude for the accretion-powered pulsations to estimate r_{bur} , using Equation (5). Although the accretion correction does make some small quantitative changes, it does not change the qualitative behaviour with energy for any of the bursts. Unless the accretion contribution differs dramatically at the time of the bursts from that observed normally, the burst fractional amplitude still falls with energy. So let us now consider the magnitude of changes to the accretion pulsations, compared to the properties measured immediately prior to each bursts, that would be necessary to mask burst pulsations whose fractional amplitude rises with energy.

If the accretion rate remains at the pre-burst level, the fractional amplitude of the accretion pulsations must fall more steeply with energy during the burst than it does normally. Either the amplitude at low energies must rise, or the amplitude at higher energies fall, or both. For most of the bursts the ratio of accretion to burst photons is less than 0.3 (Table 1). The fractional amplitude would have to change by several % RMS to have the desired effect. Whether the burst process could lead to this level of disruption is not known, but it seems unlikely. A smaller change in fractional amplitude would be required if the accretion

rate rose during a burst, boosting the ratio of accretion to burst photons. The effect of bursts on accretion rate is however unclear. Naively one might expect the radiation pressure to hinder the accretion process. But the radiation may also remove angular momentum, increasing accretion rate (Walker & Mészáros 1989; Walker 1992; Miller & Lamb 1993; Miller 1995; Ballantyne & Everett 2005). A substantial rise in accretion rate seems however unlikely, since the burst spectra are well-fit by a single temperature blackbody, and there is no spectral evidence for an enhanced accretion component.

The one-temperature hot spot models, and many of the mode models, predict burst oscillations with detectable soft lags. This could only be masked by the accretion process if the accretion-powered pulsations exhibit hard lags during bursts. This would be a reversal of the normal behaviour, requiring substantial disruption of the accretion process by the burst. Whether or not this is plausible is a topic for future study.

3.3 Hot spot with temperature gradient

The evidence presented in Strohmayer et al. (2003) and Watts, Strohmayer & Markwardt (2005) suggests that the most promising model for the burst oscillations of J1814 is a hot spot that develops at the magnetic footprint, perhaps due to a disparity in fuel build-up in this region. We will therefore focus on the hot spot model in more detail, and ask whether some simple alterations to the one-temperature hot spot models of Munro, Özel & Chakrabarty (2003) might enable us to explain the energy-dependences reported in this paper.

Although most modelling to date has focused on uniform, single temperature hot spots, several processes involved in burst generation would seem to favour some degree of temperature variation across a hot spot. For example, we expect that burning must spread in some fashion such that regions which ignite first will have a longer time to cool than portions of a hot spot which ignite later. The time asymmetry introduced by spreading can thus lead to a temperature asymmetry. Alternatively, if accretion is substantially mediated by the magnetic field, then the quantity of fuel could vary in a systematic fashion in the vicinity of the magnetic footprint. Such a fuel asymmetry could also impart a temperature gradient within the hot spot.

In order to explore the impact of a temperature gradient within a hot spot we have carried out model calculations using circular hot spots with a temperature profile across the spot. It is not our intent to fit detailed models to the data, but rather to obtain an estimate of the magnitude of a temperature gradient required to mimic the observed decrease of amplitude with energy. We use the model for emission of photons from a rotating neutron star surface described by Strohmayer (2004). The model includes bending of photon paths in a Schwarzschild geometry as well as relativistic beaming and gravitational red-shifts. Each surface element within the hot spot is assumed to emit, locally, a black body spectrum. The temperature distribution is azimuthally symmetric around the center of the hot spot, and is assumed to vary with the angle, α , measured from the central axis of the spot. For the purposes of this exploratory calculation we use a simple linear variation of the temper-

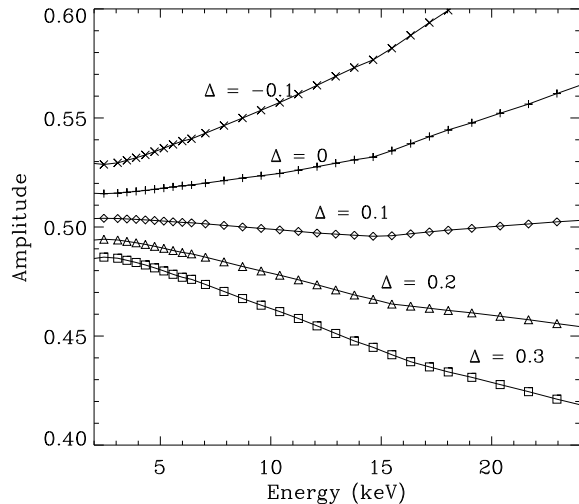


Figure 12. Rotational modulation amplitude as a function of energy for circular hot spots with a linear variation in temperature across the spot. Curves are shown for 5 different values of Δ , the fractional change in temperature from spot center to edge. The curves are labelled with the value of Δ . The uniform spot ($\Delta = 0$) has an increasing amplitude with energy, and our results confirm that an increase in temperature away from the center acts to reverse this trend, eventually producing amplitudes which fall with energy. For these calculations we used a spot size (half angle) of 90° , a location of the spot center of 80° , and an observer viewing angle of 45° (see Bhattacharyya et al. (2005), and Strohmayer (2004), for details of the modelling). The temperature at the center of the spot was 2.9 keV in each case. See the text for additional details.

ature with angle, $kT = kT_0(1 + \Delta\alpha/\alpha_0)$, where kT_0 , Δ , and α_0 are the central temperature, fractional temperature change, and angular size (half-angle) of the hot spot, respectively. We use a hot spot size and geometry consistent with the results of Bhattacharyya et al. (2005). We compute a model photon energy spectrum at infinity, and then apply an RXTE/PCA response matrix to obtain count rates versus PCA energy channel. We then compute amplitudes as a function of energy channel that can be compared with the real data. We summarize results for a range of Δ and $kT_0 = 2.9$ keV in Figure 12. We note that for these calculations we have not added a phase independent background spectrum, as was done by Bhattacharyya et al. (2005), so one should not compare directly the overall magnitude of the amplitude, just the relative change with energy.

As expected, and as shown by other authors, a uniform spot emitting a typical burst spectrum produces an increasing amplitude with energy in the PCA bandpass. Since in general a smaller hot spot produces a larger modulation amplitude one would expect that in order to produce a drop in amplitude with increasing energy the temperature should increase *away* from the center of the spot. That is, the edge should be hotter than the center. This expectation is borne out in our modeling, and we find that a fractional temperature change of 10 % from center to edge can flatten the amplitude versus energy curve for hot spot parameters plausible for J1814 (see Figure 12). In order to produce a sub-

stantial drop in amplitude with energy, variations greater than this will likely be required. Whether or not such systematic variations in temperature can actually be produced during X-ray bursts will be a subject for further study, but we note that an asymmetry associated with spreading from the center of a hot spot would tend to produce a hotter edge (as the center has longer to cool).

4 CONCLUSIONS

In this paper we have presented an analysis of the energy dependence of burst oscillations from the accreting millisecond pulsar J1814. Our results are intriguing. The fractional amplitude of the pulsations falls with energy across the 2-20 keV RXTE band; we are able to rule out the amplitude being constant, or rising with energy, at a level greater than 3σ . This mirrors the behaviour seen in the persistent accretion-powered pulsations, but differs from that seen for the burst oscillations of the non-pulsing LMXBs by Munro, Özel & Chakrabarty (2003). The persistent pulsations, like those of the other accreting millisecond pulsars, show soft lags of 0.015 cycles over the 2-20 keV band; for the burst oscillations we can rule out lags or leads of this magnitude at the 3σ level.

The energy dependence of J1814's burst oscillations differs from that reported for LMXB burst oscillations in the most comprehensive study of these objects to date (Munro, Özel & Chakrabarty 2003). It joins a list of properties that seem to differ between the two classes of objects. For the LMXBs, bursts are only seen at high accretion rate; for the pulsars bursts are seen even though the accretion rate never gets high (Munro, Galloway & Chakrabarty 2004). LMXB burst oscillations show frequency shifts of up to 5Hz (see for example Munro et al. (2001)); for the pulsars frequency variation is only seen in the rises of those bursts that show PRE (Chakrabarty et al. 2003; Watts, Strohmayer & Markwardt 2005). The LMXB burst oscillations also show amplitude variations (Munro, Özel & Chakrabarty 2002); for J1814 no such variations are seen except during PRE (Watts, Strohmayer & Markwardt 2005). Finally, the pulsar burst oscillations have detectable harmonic content (Chakrabarty et al. 2003; Strohmayer et al. 2003), whereas the LMXB oscillations do not (Munro, Özel & Chakrabarty 2002).

The differing properties suggest that the mechanism responsible for the burst oscillations may differ between the two classes of objects. Further study, however, is clearly required. There is now a much larger sample of LMXB burst oscillations in the RXTE archive, and it would be advisable to check whether the trends found in the studies by Munro and collaborators still hold for a larger sample. The energy dependence of the burst oscillations of the accreting millisecond pulsar J1808 also remains to be analysed. Our study also highlights the need to look at variations in properties over the course of the outburst; both accretion-powered and burst oscillation properties were found to vary for J1814. The technique of folding together multiple bursts, for example (used both in this paper and in the previous study by Munro, Özel & Chakrabarty (2003)), could obscure interesting variations.

The drop in fractional amplitude with energy observed in the burst oscillations of J1814 is inconsistent with the predictions of both surface mode and one-temperature hot spot models. If these models are correct then there must be substantial changes in the accretion process, triggered by the burst, that cause the accretion pulsations to mask this property of the thermonuclear pulsations. If we assume that the accretion process does not alter significantly during the burst then we must seek an alternative theory. One possibility is that the hot spot possesses a temperature gradient. In Section 3.3 we examined the magnitude of the gradient that might be required to explain the observations. It is substantial: a rise of more than 10% rise from center to edge. How such a gradient might be generated is an interesting theoretical question that we hope to address in future work. Other processes such as beaming due to a corona, however, may have to be invoked to explain the observations.

5 ACKNOWLEDGMENTS

We are grateful to Tony Piro for encouraging us to look at this issue, and to Craig Markwardt for providing the orbital ephemeris for XTE J1814-338. ALW acknowledges partial support from the European Union FP5 Research Training Network 'Gamma-Ray Bursts: An Enigma and a Tool'. This research has made use of data obtained from the High Energy Astrophysics Science Archive Research Center (HEASARC) provided by NASA's Goddard Space Flight Center.

REFERENCES

- Ballantyne D.R., Everett J.E., 2005, *ApJ*, 626, 364
- Bhattacharyya S., Strohmayer T.E., Miller M.C., Markwardt, C.B., 2005, *ApJ*, 619, 483
- Brainerd C.B., Lamb, F.K., 1987, *ApJ*, 317, L33
- Buccheri R. et al., 1993, *A&A*, 128, 245
- Chakrabarty D., Morgan E.H., Munro M.P., Galloway D.K., Wijnands R., van der Klis M., Markwardt, C.B., 2003, *Nature*, 424, 42
- Cui W., Morgan E.H., Titarchuk L.G., 1998, *ApJ*, 504, L27
- Cumming A., 2005, *ApJ*, 630, 441
- Cumming A., Zweibel E., Bildsten L., 2001, *ApJ*, 557, 958
- Ford E.D., 2000, *ApJ*, 535, L19
- Galloway D.K., Chakrabarty D., Morgan E.H., Remillard R.A., 2002, *ApJ*, 576, L137
- Galloway D.K., Markwardt C.B., Morgan E.H., Chakrabarty D., Strohmayer T.E., 2005, *ApJ*, 622, L45
- Gierliński M., Done C., Barret D., 2002, *MNRAS*, 331, 141
- Gierliński M., Poutanen J., 2005, *MNRAS*, 359, 1261
- Gilfanov M., Revnivtsev M., Sunyaev R.A., Churazov E., 1998, *A&A*, 338, L83
- Groth E.J., 1975, *ApJSS*, 29, 285
- Heyl J., 2004, *ApJ*, 600, 939
- Heyl J., 2005, *MNRAS*, 361, 504
- Kirsch M.G.F., Mukerjee K., Breittellner M.G., Djavidnia S., Freyberg M J., Kendziorra E., Smith M.J.S., 2004, *A&A*, 423, L9
- Krauss M.I. et al., 2005, *ApJ*, 627, 910

- Kylafis N.D., Klimmis G.S., 1987, ApJ, 323, 678
Lee U., 2004, ApJ, 600, 914
Lee U., Strohmayer T.E., 2005, MNRAS, 558
Markwardt C.B., Swank J.H., 2003, IAU Circ., 8144, 1
Markwardt C.B., Strohmayer T.E., Swank J.H., 2003, Atel
164
McDermott P.N., Taam R.E., 1987, ApJ, 318, 278
Mészáros P., Riffert H., Berthiaume G., 1988, ApJ, 325,
204
Miller M.C., 1995, ApJ, 441, 770
Miller M.C., Lamb F.K., 1993, ApJ, 413, L43
Muno M.P., Chakrabarty D., Galloway D.K., Psaltis D.,
2001, ApJ, 580, 1048
Muno M.P., Özel F., Chakrabarty D., 2002, ApJ, 581, 550
Muno M.P., Özel F., Chakrabarty D., 2003, ApJ, 595, 1066
Muno M.P., Galloway D.K., Chakrabarty D., 2004, ApJ,
608, 930
Piro A.L., Bildsten L., 2005, ApJ, 629, 438
Piro A.L., Bildsten L., 2006, ApJ, 638, 968
Poutanen J., Gierliński M., 2003, MNRAS, 343, 1301
Sazunov S.Y., Sunyaev R.A., 2001, A&A, 373, 241
Spitkovsky A., Levin Y., Ushomirsky G., 2002, ApJ, 566,
1018
Strohmayer T.E., 2004, in Kaaret P., Lamb F.K., Swank
J.H., eds, AIP Conf. Proc. Vol. 714, X-ray Timing 2003:
Rossi and Beyond, Melville, New York, p.245
Strohmayer T.E., Bildsten L., 2006, in Lewin W.H.G., van
der Klis M., eds, Compact Stellar X-ray Sources, Cam-
bridge University Press
Strohmayer T.E., Markwardt C.B., 2002, ApJ, 577, 337
Strohmayer T.E., Markwardt C.B., 2002, ApJ, 581, 577
Strohmayer T.E., Zhang W., Swank J.H., Lapidus I., 1998,
ApJ, 503, L147
Strohmayer T.E., Markwardt C.B., Swank J.H., in't Zand
J.J.M., 2003, ApJ, 596, L67
Titarchuk L.G., Cui W., Wood K., 2002, ApJ, 576, L49
Vaughan B.A. et al., 1994, ApJ, 435, 362
Walker M.A., 1992, ApJ, 385, 642
Walker M.A., Mészáros P., 1989, ApJ, 346, 844
Watts A.L., Strohmayer T.E., Markwardt C.B., 2005, ApJ,
634, 547
Wood K.S., Ftaclas C., Kearney M., 1988, ApJ, 324, L63

Table 1. **Summary of burst properties.** Photon ratios (columns 5-7) and accretion-corrected amplitudes (columns 8-10) are calculated assuming accretion rate and pulsation properties remain at pre-burst levels. No error bars are given for columns 8-10 because of the uncertainties inherent in this assumption: the error bars in columns 2-4 should be taken as a lower limit.

Index	RMS fractional amplitude (%)			$N_{\text{acc}}/N_{\text{bur}}$			Accretion-corrected amplitudes		
	2-5 keV	5-10 keV	10-20 keV	2-5 keV	5-10 keV	10-20 keV	2-5 keV	5-10 keV	10-20 keV
1	8.4 ± 0.7	8.0 ± 0.7	$5.6^{+1.7}_{-1.3}$	0.24	0.31	0.78	7.9	7.5	1.5
2	9.8 ± 0.6	9.9 ± 0.5	11.0 ± 1.0	0.11	0.09	0.15	9.8	10.0	11.3
3	11.4 ± 0.6	9.8 ± 0.5	$8.3^{+1.0}_{-0.9}$	0.15	0.09	0.17	11.6	9.8	8.1
4	10.3 ± 0.5	10.0 ± 0.4	8.7 ± 0.8	0.19	0.11	0.14	10.3	10.0	8.5
5	11.6 ± 0.8	10.8 ± 0.6	$10.2^{+1.2}_{-1.0}$	0.17	0.12	0.19	11.7	10.9	10.4
6	9.6 ± 0.8	9.1 ± 0.8	$8.5^{+1.6}_{-1.4}$	0.35	0.34	0.89	8.9	8.5	6.9
7	11.8 ± 0.5	11.0 ± 0.4	10.5 ± 0.9	0.20	0.14	0.20	11.9	11.1	10.6
8	12.2 ± 0.7	11.0 ± 0.7	$10.6^{+1.6}_{-1.4}$	0.31	0.34	0.67	12.3	11.2	10.8
9	9.0 ± 0.7	8.9 ± 0.6	$7.8^{+1.4}_{-1.2}$	0.21	0.23	0.41	8.3	8.4	6.7
10	12.7 ± 0.5	11.3 ± 0.4	8.8 ± 0.9	0.19	0.16	0.22	12.8	11.3	8.4
11	11.0 ± 0.5	11.4 ± 0.5	9.2 ± 0.9	0.18	0.12	0.22	10.8	11.4	8.9
12	11.4 ± 0.5	11.2 ± 0.4	10.1 ± 0.9	0.19	0.14	0.26	11.3	11.1	9.9
13	14.1 ± 0.6	11.0 ± 0.5	10.5 ± 0.9	0.14	0.17	0.33	14.4	10.9	10.4
14	11.1 ± 1.0	11.5 ± 1.0	$8.9^{+2.6}_{-2.0}$	0.26	0.26	0.51	10.9	11.5	7.8
15	11.7 ± 0.5	11.7 ± 0.4	10.0 ± 0.8	0.17	0.13	0.23	11.8	11.8	10.1
16	11.5 ± 0.6	11.2 ± 0.5	$8.2^{+1.0}_{-0.9}$	0.16	0.14	0.18	11.4	11.2	7.9
17	11.4 ± 0.5	11.1 ± 0.5	10.5 ± 0.9	0.20	0.13	0.24	11.4	11.1	10.6
18	11.4 ± 0.5	10.8 ± 0.4	9.3 ± 0.8	0.13	0.11	0.14	11.4	10.8	9.3
19	11.7 ± 0.8	10.8 ± 0.8	$8.5^{+2.0}_{-1.6}$	0.41	0.44	0.58	11.9	10.9	8.1
20	10.7 ± 0.6	10.5 ± 0.5	$7.3^{+1.0}_{-0.8}$	0.17	0.12	0.15	10.6	10.4	6.9
21	12.1 ± 0.6	11.0 ± 0.5	$9.0^{+1.0}_{-0.9}$	0.13	0.12	0.22	12.1	11.1	9.0
22	12.1 ± 0.5	11.7 ± 0.4	10.1 ± 0.8	0.20	0.16	0.27	12.2	11.7	10.0
23	11.7 ± 0.6	11.5 ± 0.5	9.7 ± 0.9	0.11	0.09	0.18	11.6	11.5	9.5
24	12.2 ± 0.6	12.0 ± 0.5	$8.2^{+1.0}_{-0.9}$	0.16	0.13	0.23	12.1	12.1	7.6
25	11.5 ± 0.7	11.4 ± 0.6	$9.7^{+1.2}_{-1.1}$	0.21	0.14	0.28	11.4	11.4	9.6
26	10.9 ± 0.5	11.8 ± 0.4	11.0 ± 0.8	0.14	0.11	0.30	10.8	11.8	10.8
27	11.4 ± 0.5	10.7 ± 0.5	11.4 ± 1.0	0.19	0.10	0.23	11.1	10.5	11.0
28	$3.8^{+0.6}_{-0.5}$	$3.9^{+0.5}_{-0.4}$	$1.9^{+1.0}_{-0.7}$	0.04	0.02	0.02	3.5	3.7	1.8